



# In situ solid-state NMR of a magnetically oriented microcrystal suspension



Ryosuke Kusumi<sup>a,\*</sup>, Hiroshi Kadoma<sup>a</sup>, Masahisa Wada<sup>a,b</sup>, Kazuyuki Takeda<sup>c</sup>, Tsunehisa Kimura<sup>a,d</sup>

<sup>a</sup> Division of Forest and Biomaterials Science, Graduate School of Agriculture, Kyoto University, Kyoto 606-8502, Japan

<sup>b</sup> College of Life Science, Kyung Hee University, Yongin-si, Gyeonggi-do 446-701, Republic of Korea

<sup>c</sup> Division of Chemistry, Graduate School of Science, Kyoto University, Kyoto 606-8502, Japan

<sup>d</sup> Fukui University of Technology, 3-6-1 Gakuen, Fukui 910-8505, Japan

## ARTICLE INFO

### Article history:

Received 8 August 2019

Revised 25 September 2019

Accepted 8 October 2019

Available online 10 October 2019

### Keywords:

Magnetically oriented microcrystal suspension (MOMS)

In situ measurement

Chemical shift anisotropy

Single-crystal rotation pattern

## ABSTRACT

In situ solid-state NMR measurements of a magnetically oriented microcrystal suspension (MOMS) were demonstrated. Under modulated rotation of the static field, or equivalently, of the sample tube, randomly oriented microcrystals in a viscous liquid medium feel a torque arising from the anisotropic bulk susceptibility and eventually aligned in the same direction. In this way, a three-dimensional MOMS (3D-MOMS) was obtained. To apply an elliptically rotating magnetic field to microcrystals in suspension, a probe to rotate the sample tube around an axis perpendicular to the static magnetic field was developed. Single-crystal (SC) rotation patterns were obtained from the 3D-MOMS by solid-state CP measurements triggered in synchronous with the sample-tube rotation. Unlike the traditional SC method, the 3D-MOMS approach presented here does not require the elaborate adjustment of the direction of the reference frame. The process of three-dimensional magnetic alignment was also studied by monitoring the spectral changes during continuous application of the modulated sample rotation.

© 2019 Elsevier Inc. All rights reserved.

## 1. Introduction

The chemical shift (CS) tensor provides information about the electron distribution around the nucleus being observed. The single-crystal (SC) rotation method [1,2], in which patterns of the changes of the observed chemical shifts are measured as a function of the rotation angle of a single crystal (rotation pattern), offers an accurate and direct means to determine the CS tensor with respect to the unit cell. Other tensors related to NMR phenomena, such as quadrupolar interaction, can also be completely determined using the SC method [3]. A two-dimensional SC method for a complex single crystal has also been proposed [4,5]. However, these direct methods can be used only when a relatively large single crystal with a size of several millimeters is available. Although the combination of microcoil detectors [6] with SC magic angle spinning (MAS) [7] can provide comprehensive information about the anisotropic tensors for small crystals of sub-millimeter size [6,8], the measurements may be time-consuming. In addition, it is difficult to apply the technique to smaller crystals (<100 μm) because the crystal has to be inserted precisely into a rotor with an axis of the reference frame, e.g., a crystal axis, parallel to the rotor axis.

Moreover, the measurement of such a small single crystal can suffer from low sensitivity.

We recently succeeded in determining the CS tensors for microcrystalline powder samples through the formation of magnetically oriented microcrystal arrays (MOMAs) [9–11]. A MOMA is a composite in which microcrystals align three-dimensionally in a polymer matrix [12]. When microcrystals dispersed in a liquid medium are exposed to a frequency-modulated rotating magnetic field [13], three-dimensional (3D) alignment of the microcrystals can occur to form a magnetically oriented microcrystal suspension (MOMS). After polymerization of the medium, a MOMA is obtained as a “pseudo single crystal”. We showed that the combination of a MOMA and the traditional SC rotation method provided not only the principal values but also the orientations of the principal axes with respect to the crystallographic axes. It should be noted that the CS tensor was fully determined from microcrystals that were just tens of micrometers in size [9]. This approach has very high sensitivity because the total volume of microcrystals in a MOMA is equal to or larger than that of a single crystal of millimeter size. However, this combined method has some drawbacks: the orientation fluctuation of microcrystals in a MOMA produced via solidification of the matrix liquid is large; once consolidated, microcrystals cannot be recycled; and precise setting of the MOMA

\* Corresponding author.

E-mail address: [r\\_kusumi@kais.kyoto-u.ac.jp](mailto:r_kusumi@kais.kyoto-u.ac.jp) (R. Kusumi).

into a goniometer probe to measure SC rotation patterns is complicated.

To overcome the above drawbacks, here we develop a probe for in situ solid-state NMR of a MOMS. The probe allows the SC rotation pattern to be obtained from a microcrystal suspension oriented in an NMR magnet without solidification of the suspending medium. We prepare a MOMS of L-alanine by frequency-modulated rotation under a 7-T static magnetic field and then conduct NMR measurements during sample rotation with an incremental delay, yielding the SC rotation pattern. The changes in the spectral pattern during the 3D alignment process are also studied.

## 2. Theory: 3D orientation of microcrystals under an elliptical magnetic field

Here, we briefly describe the basic concept of 3D alignment under dynamic magnetic fields; further details have been reported elsewhere [14]. Crystals and microcrystals, whether organic or inorganic, can be magnetically oriented provided that they have diamagnetic anisotropy. The magnetic susceptibility tensor  $\chi$  of a crystal is characterized by three principal values ( $\chi_1 \geq \chi_2 \geq \chi_3$ ) and the corresponding principal axes. Under a static magnetic field  $\mathbf{B}$ , the  $\chi_1$ -axis (easy magnetization axis) of the crystal is uniaxially aligned along the  $\mathbf{B}$  direction. In contrast, uniaxial orientation of the  $\chi_3$ -axis (hard magnetization axis) is induced under a rotating magnetic field. For biaxial crystals such as those in orthorhombic, monoclinic, and triclinic systems, the 3D orientation of the principal axes occurs under an elliptically rotating magnetic field because all the principal values are different. Several types of dynamic magnetic fields have been reported [14,15] since the original work by Staines [16,17], including amplitude-modulated [13,15], frequency-modulated [12,18], intermittently rotating [18], and oscillating [19] magnetic fields. When performing orientation experiments, the sample is rotated or oscillated in a static magnetic field rather than moving the magnetic field around the fixed sample.

In the present study, we used an intermittently rotating magnetic field [18], as schematically illustrated in Fig. 1. In our experiments, a microcrystal suspension was intermittently rotated in a static magnetic field  $\mathbf{B}$  instead of rotating the magnetic field. Here,  $x, y, z$  and  $x', y', z'$  represent the coordinates in the laboratory and sample-tube frames, respectively. The latter coordinate system fixed in the sample-tube is defined to describe the intermittent rotation of the suspension and the orientation of microcrystals under the magnetic fields. The sample rotation axis ( $x'$ -axis|| $x$ -axis) was perpendicular to the  $\mathbf{B}$  direction ( $z$ -axis), and the initial position of the  $z'$ -axis was defined to be located on the  $z$ -axis. The sample tube was rotated about the  $x'$ -axis but the  $z'$ -axis temporarily stopped in the  $z$ -axis (|| $\mathbf{B}$ ) for a time period of  $t_s$  every 180° rotation. The rotation speed  $\omega_r$  was set to be high enough to satisfy the condition of  $\omega_r \tau \gg 1/2$ , which is referred to as the rapid rotation regime (RRR) [14,20]. Here,  $\tau$  is the intrinsic orientation time, which is defined as [14,20]

$$\tau = 6\mu_0\eta / (F(D)\chi_a B^2) \quad (1)$$

where  $\mu_0$  is the magnetic permeability of vacuum,  $\eta$  is the viscosity of the medium, and  $\chi_a$  is the magnetic anisotropy given by  $K_1(\chi_2 - \chi_3)$ ,  $K_2(\chi_1 - \chi_3)$ , or  $K_3(\chi_1 - \chi_2)$ . Here,  $K_1$ ,  $K_2$ , and  $K_3$  are constants, as defined in reference 14.  $F(D)$  is unity in the limit of a sphere ( $D = 1$ ) [21,22]. The motion of a microcrystal in a viscous medium under a dynamic magnetic field is described by the balance of magnetic and hydrodynamic torques [14,20]. Analysis of the differential equation of the motion of magnetically uniaxial crystal (for example,  $\chi_2 = \chi_3$  and  $\chi_a = \chi_1 - \chi_3$ ) under a rotating magnetic field shows the  $\chi_1$ -axis rotates synchronously with the

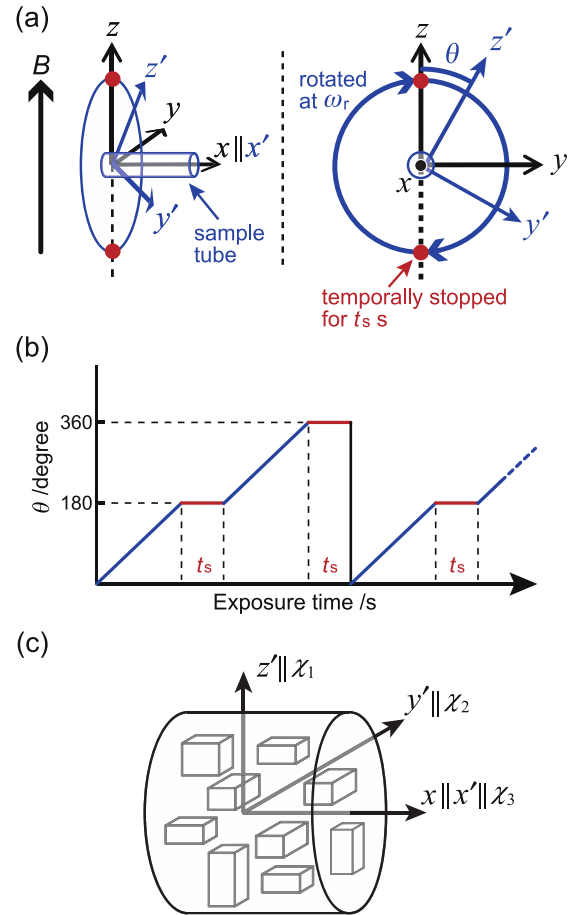


**Fig. 1.** Schematics of (a) the application of an intermittently rotating magnetic field, (b) the change of the rotation angle  $\theta$  under the intermittent rotation, and (c) the 3D orientation of microcrystals achieved under the modulated magnetic field.

magnetic rotation when the rotation speed is slow ( $\omega_r \tau < 1/2$ ). This condition is referred to as a synchronous rotation regime (SRR) [14,20]. Under the SRR condition, on the other hand, the  $\chi_1$ -axis cannot follow the rotation of the magnetic field  $\mathbf{B}$  while  $\chi_3$ -axis aligns perpendicular to the rotating field due to the time-averaged magnetic energy over one revolution of the magnetic field. A simple rotation under a static magnetic field at a higher constant rate (RRR condition) induces uniaxial alignment of  $\chi_3$ -axis perpendicular to the  $yz$  plane. It is expected that the  $\chi_1$ -axis of biaxial crystal behaves similarly. Under the intermittent mode that satisfies the RRR condition, the  $\chi_3$ -axis of the crystal aligns in the direction of the  $x'$ -axis ( $\perp yz$  plane). Simultaneously, the  $\chi_1$ -axis also aligns in the  $z'$ -direction because the crystal is temporarily exposed to the static magnetic field for  $t_s$  when the  $z'$ -axis is directed to the  $\mathbf{B}$  direction. The tube rotation should be stopped exactly in the  $\mathbf{B}$  direction to reduce the orientation fluctuation of the  $\chi_1$ -axis. The appropriate combination of  $t_s$  and  $\omega_r$  depends on samples. We can optimize the condition to achieve 3D alignment with lower orientation fluctuation if the  $\chi_a$  is known [14]. When the information for  $\chi_a$  is unavailable, we should optimize the parameters through evaluation of the peak width with different conditions.

This 3D alignment is maintained under the continuous application of the intermittently rotating magnetic field, whereby the microcrystals rotate synchronously with the sample tube rotation. This intermittent-type magnetic field is appropriate for the present in situ NMR measurements because the detection and accumulation of FID can be easily performed as the sample tube is rotated.

The 3D oriented microcrystal suspension obtained under the intermittent rotating magnetic field is referred to as a 3D-MOMS and the uniaxially oriented microcrystal suspensions under static and rotating magnetic fields are denoted as 1D-MOMSs.

### 3. Experimental

#### 3.1. Experimental setup for in situ solid-state NMR of MOMS

A probe to measure the solid-state NMR spectra of the MOMSs was developed based on a 7.0-mm double-resonance MAS probe. Fig. 2 shows photographs and schematics of the developed probe. The probe was designed such that the rotation axis of the sample tube ( $x'$ -axis in Fig. 1(a)) was perpendicular to the static magnetic field  $B_0$  used for NMR. The solenoid coil had an inner diameter of 9.0 mm to house the sample tube with a diameter of 8.0 mm. The modulated rotation of the tube was controlled by a stepping motor outside the magnet via drive shafts. The  $\omega_r$  could be changed from 1.2 to 200 rotations per minute (rpm). The  $z'$ -direction of the tube was accurately monitored by a photosensor so that the NMR measurements could be performed synchronously with the sample-tube rotation. The probe was connected to an OPEN-CORE NMR spectrometer [23] equipped with a power amplifier (JEOL CMX300 Infinity). All in situ solid-state NMR measurements were performed in a 7.05-T superconducting magnet.

#### 3.2. In situ solid-state NMR measurements of a MOMS

As-received L-alanine (Wako Pure Chemical Industries, Ltd., Osaka, Japan) was pulverized with a mortar and pestle. After being passed through a 20-mesh sieve to remove the larger crystals, the microcrystalline powder (<20  $\mu\text{m}$ ) was dispersed in UV-curable acrylate XVL-14 (Kyoritsu Chemical & Co., Ltd., Tokyo, Japan; viscosity of 12 Pa s). Note that we used the resin not for UV-curing the sample but because of the viscosity high enough to achieve the RRR condition (see Eq. (1)). Another viscous medium, e.g., a viscous polymer solution, can be used as an alternative as far as the RRR condition is satisfied. The weight fraction of microcrystals was ca. 25%. It should be pointed out that the higher concentration of crystals in a suspension results in the lower degree of orientation; it is desirable that the weight fraction is kept within 30% from the view point of the balance between signal to noise ratio and linewidth of resonance peaks. A polychlorotrifluoroethylene tube

with an inner diameter of 5.5 mm and inner height of 32 mm was filled with the suspension. The sample tube was mounted on the probe and inserted into the superconducting magnet. The other parameters for  $^{13}\text{C}$  cross polarization (CP) measurements were as follows:  $^1\text{H}$  resonance frequency, 298.6 MHz;  $^1\text{H}$   $\pi/2$  pulse width, 3.25  $\mu\text{s}$ ; contact time, 1 ms; recycle delay, 6 s. A total of 2048 scans was accumulated at each rotation angle  $\theta$ . The  $^{13}\text{C}$  CP/MAS spectrum of the microcrystalline powder was obtained using a 400-MHz VNMRS spectrometer (Varian, Inc., Palo Alto, California, USA) equipped with a 4.0-mm double-resonance MAS probe under the following conditions: MAS frequency, 15 kHz;  $^1\text{H}$  and  $^{13}\text{C}$   $\pi/2$  pulse widths, 2.8 and 2.6  $\mu\text{s}$ , respectively; CP contact time, 1 ms; recycle delay, 5 s; accumulated number of scans, 512.

#### 3.3. Observation of 3D magnetic alignment under a modulated magnetic field

The spectral change caused by the 3D alignment of microcrystals in a suspension under the intermittently rotating magnetic field was observed for  $^{13}\text{C}$ -labeled L-alanine. L-Alanine ( $1\text{-}^{13}\text{C}$ , 99%, Cambridge Isotope Laboratories, Inc. (Andover, MA, USA)), of which carboxyl carbons are labeled with  $^{13}\text{C}$ , was used after recrystallization. The obtained crystals were pulverized with a mortar and pestle and then dispersed in the UV-curable monomer at a weight fraction of 20%. The suspension was allowed to stand for 3 days to form a lower layer of large crystals and upper layer of small ones. A small amount of the suspension was taken from between these two layers and poured into the sample tube. The sample tube was mounted on the probe and inserted into the magnet. After sitting without rotation for 30 min to achieve uniaxial alignment of microcrystals, the intermittent rotation was started. The  $^{13}\text{C}$  solid-state CP spectra of  $\theta = 90^\circ$  and  $270^\circ$  were continuously collected in a single scan. The recycle delay was 3 s.

#### 3.4. Simulations

The  $^{13}\text{C}$  solid-state NMR spectra of the 1D- and 3D-MOMSs were simulated from the single-crystal data for L-alanine [24,25]. The spectral simulations were performed on Mathematica 11 (Wolfram Research, Inc., Champaign, IL, USA). The theoretical  $^{13}\text{C}$  peaks were convoluted with a Gaussian function with a full width at half maximum (FWHM) of 17 ppm. The quadrupole interaction with  $^{14}\text{N}$  nuclei was not considered for the simulated peaks of  $\text{C}\alpha$  carbons.

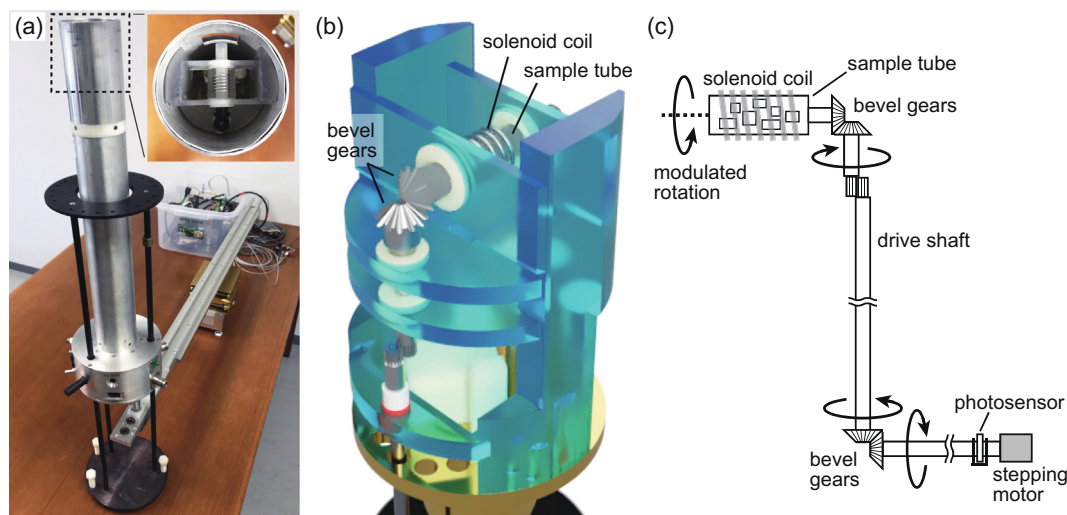


**Fig. 2.** (a) Photographs and (b), (c) schematics of the probe developed for in situ solid-state NMR measurements of the MOMSs. The inset in (a) shows a photograph around the rf coil.

## 4. Results and discussion

### 4.1. In situ $^{13}\text{C}$ CP spectra of 1D-MOMs

Fig. 3(a) and (b) show  $^{13}\text{C}$  solid-state CP NMR spectra obtained for a polycrystalline sample of L-alanine under MAS at 15 kHz and static conditions, respectively. As expected, MAS gave narrow resonance lines at the positions of the isotropic chemical shifts, whereas the powder pattern reflecting the CS tensors was obtained for the static sample. To demonstrate 1D-MOMS, we set the microcrystal dispersion of L-alanine into the probe, and left the sample in the 7-T magnet for 30 min. Then, we performed  $^{13}\text{C}$  CP measurements, and obtained the spectrum shown in Fig. 3(c). Here, the relationship between the magnetization axes ( $\chi_1 > \chi_2 > \chi_3$ ) and crystallographic axes of L-alanine is known to be  $\chi_1 \parallel c$ ,  $\chi_2 \parallel a$ , and  $\chi_3 \parallel b$  [12]. The  $\chi_1$ -axis (*c*-axis) of the L-alanine crystals should be aligned parallel to  $B_0$ , while the other axes are randomly oriented around  $B_0$ . Indeed, the NMR spectrum in Fig. 3(c) was reproduced by a calculated pattern for uniaxial alignment along the *c*-axis using the single-crystal data for L-alanine [24], as illustrated by the dashed line in Fig. 3(c). In contrast to the  $\chi_1$ -axis alignment realized for the stationary sample, the  $\chi_3$ -axis can be aligned by rotating the sample at a constant rate, i.e., without modulation, around an axis perpendicular to  $B_0$ , as demonstrated in Fig. 3(d). Here, the NMR signal was acquired without stopping sample rotation. Because the period of signal acquisition was much shorter than the rotation period, the effect of sample tilting during acquisition was negligible. The dashed line in Fig. 3(d) represents the resonance line calculated for the  $\chi_3$ -axis (*b*-axis) alignment, which agrees well with the experimental spectrum.

It should be noted that the microcrystals aligned in a coordinate system fixed in the sample tube. For the special case of the uniaxial alignment along the sample-rotation axis demonstrated above, the profile of the resonance line was independent of the phase of the rotor at which the implementation of the pulse sequence was triggered. Conversely, in the case of complete 3D alignment by modulated rotation,  $\theta$  of the rotor at the time of signal acquisition affects the orientation of the microcrystals with respect to the static field.

Thus, by acquiring signals for various values of  $\theta$ , a set of spectra corresponding to the SC rotation pattern can be obtained.

### 4.2. In situ measurements of single-crystal rotation patterns of a 3D-MOMS

In 3D-MOMS experiments, intermittent rotation was applied by rotating the sample at 15 rpm among  $180^\circ$  rotation with a pause of 1 s every  $180^\circ$  rotation. That is, a cycle of rotation at a speed of  $90^\circ/\text{s}$  for 2 s followed by a pause of 1 s was repeated for 30 min before NMR measurements. The  $\theta$  angle was changed by  $\Delta\theta$  induced by shifting the timing of the NMR pulse by  $\Delta t = \Delta\theta/\omega$ . Within this period, the  $\chi_1$ -axis continues to rotate by  $\Delta\theta$  if the RRR condition is satisfied. By using the values of  $\mu_0 = 4\pi \times 10^{-7} \text{ H/m}$ ,  $B = 7.05 \text{ T}$ ,  $\eta = 12 \text{ Pa s}$ ,  $F(D) = 1$ ,  $\chi_a = 1.0 \times 10^{-7} (= K_1(\chi_2 - \chi_3))$  where  $K_1 = 1/3$  and  $\chi_2 - \chi_3 = 3.0 \times 10^{-7}$  [26], and  $\omega_r = 15 \text{ rpm}$ , we obtain  $\omega_r \tau = 28.6 \gg 1/2 \text{ rad}$ , which satisfies the RRR condition. Fig. 4 presents the  $^{13}\text{C}$  solid-state CP NMR spectra obtained for a 3D-MOMS of L-alanine with different  $\theta$ . The peak positions varied systematically depending on  $\theta$ . Furthermore, the peak positions in each spectrum coincided with those of the corresponding spectrum for L-alanine calculated from the single-crystal data [24]. These results indicate that the SC rotation patterns, which usually require a large single crystal, were successfully obtained from the microcrystalline powder aligned three-dimensionally in a liquid medium using the in situ MOMS probe developed in this study.

### 4.3. Spectral changes during the magnetic alignment process under the modulated rotating magnetic field

To monitor the process of complete alignment of the L-alanine microcrystals, we traced the change in the NMR spectrum under the intermittently rotating magnetic field. The solid-state  $^{13}\text{C}$  CP spectra collected at  $\theta = 90^\circ$  and  $270^\circ$  are depicted in Fig. 5 at an enlarged scale between 50 and 260 ppm (COO<sup>-</sup> region). Before starting the intermittent rotation ( $t = 0 \text{ s}$ ), the sample was left stationary for a sufficiently long time, and we made sure that the

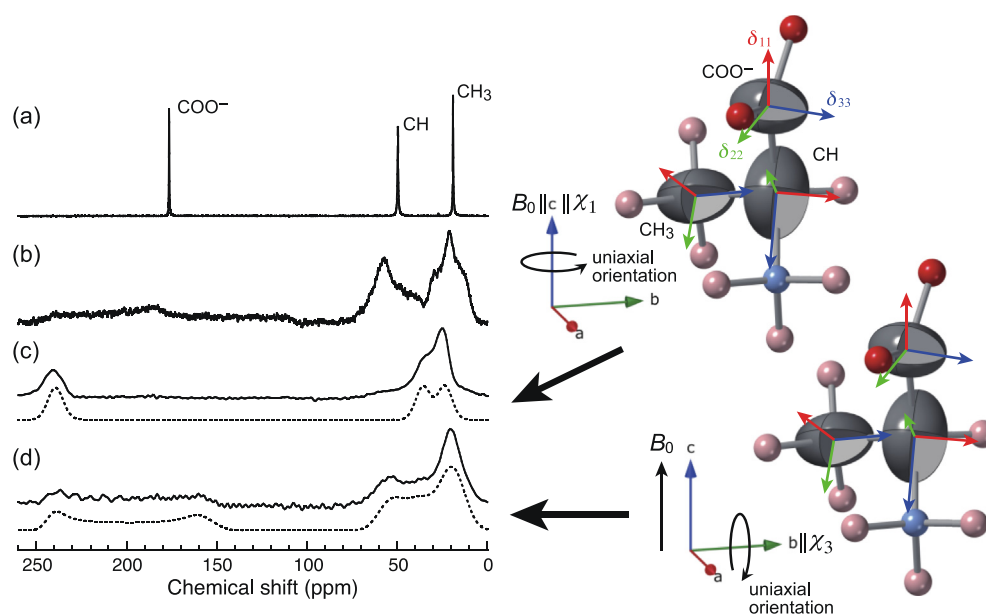


**Fig. 3.**  $^{13}\text{C}$  solid-state CP NMR spectra of L-alanine microcrystals (a) with MAS (15 kHz), (b) without MAS, (c) in a suspension under a static magnetic field, and (d) in a suspension under a rotating magnetic field (15 rpm). The spectra calculated from the single-crystal data for L-alanine [24] assuming uniaxial orientation under each magnetic field are also shown as dashed lines. The ellipsoids of  $^{13}\text{C}$  CS tensors are depicted for an L-alanine molecule I ( $l, m, n$ ) in the unit cell. The other three molecules, which are related by the symmetry operation I ( $-l, -m, n$ ), III ( $l, -m, -n$ ), and IV ( $-l, m, -n$ ), exhibit the same spectral pattern under each magnetic field.

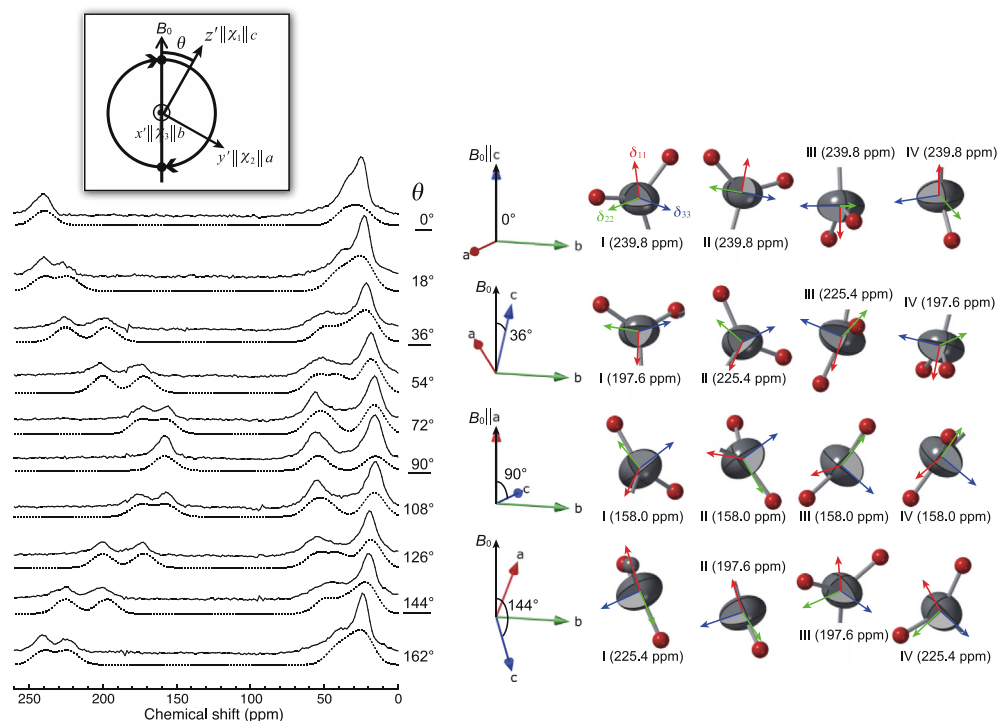


**Fig. 4.** In situ  $^{13}\text{C}$  solid-state CP NMR spectra of a 3D-MOMS of L-alanine, where  $\theta$  is the angle between the  $\chi_1$ -axis and static field  $B_0$  at the moment when signal acquisition was triggered. The  $^{13}\text{C}$  CS tensors of  $\text{COO}^-$  groups are also illustrated for four magnetically nonequivalent molecules in the unit cell at  $\theta = 0^\circ, 36^\circ, 90^\circ$ , and  $144^\circ$ , together with the CS values calculated assuming each orientation of the crystal under the intermittently rotating magnetic field.

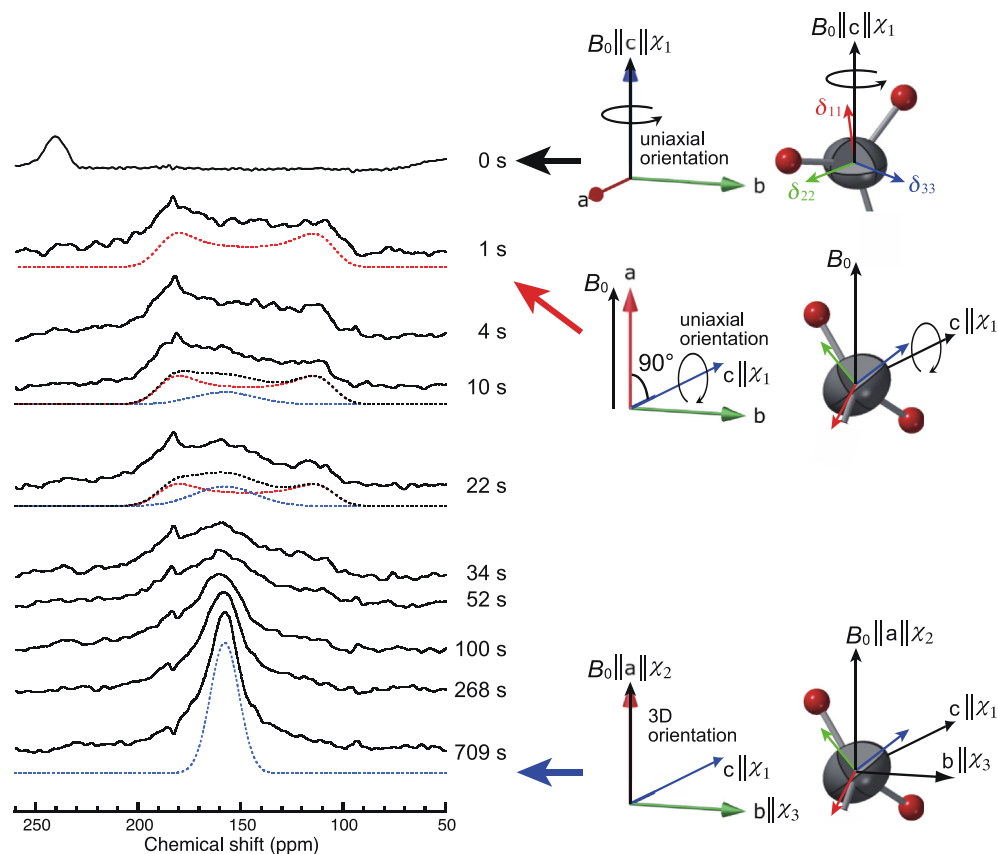


**Fig. 5.** In situ solid-state  $^{13}\text{C}$  CP spectra collected at  $\theta = 90^\circ$  and  $270^\circ$  with a single scan. An enlarged scale of the spectra in the  $\text{COO}^-$  region is shown. The red and blue dotted lines indicate the resonance peaks simulated assuming the uniaxial orientation of  $\chi_1$ -axes perpendicular to  $B_0$  and the 3D orientation of the magnetic susceptibility axes, respectively. The  $^{13}\text{C}$  CS tensors of  $\text{COO}^-$  groups are also illustrated for an L-alanine molecule  $l$  ( $l, m, n$ ) in the unit cell. (For interpretation of the references to colour in this figure legend, the reader is referred to the web version of this article.)

resonance line, as shown at the top of Fig. 5, exhibited the shape corresponding to the uniaxial orientation of the  $\chi_1$ -axis along  $\mathbf{B}_0$ . Then, we started the intermittent rotation in the same way as that used to obtain the spectra in Fig. 4. The  $^{13}\text{C}$  FIDs were separately acquired at the time when  $\theta$  became  $90^\circ$  and  $270^\circ$ , so that the spectra at times of  $(3k + 1)$  s ( $k = 0, 1, 2, \dots$ ) were obtained.

The change in the spectrum after 1 s from the start of the intermittent rotation was simply ascribed to the flip of the  $\chi_1$ -aligned MOMS by  $90^\circ$ , which resulted in the uniaxial orientation of the  $\chi_1$ -axes perpendicular to  $\mathbf{B}_0$ , as verified by a simulation (red dotted line in Fig. 5). After 10 s, the spectra exhibited unique patterns consistent with the superposition of that for the  $\chi_1$ -uniaxial orientation and that for the full orientation of the  $\chi_1, \chi_2$ , and  $\chi_3$ -axes (blue dotted line). The fraction of the latter increased with the time of intermittent rotation, reflecting the progress of the 3D orientation of the microcrystals. After longer application of the intermittent rotation ( $>100$  s), the spectral pattern became that of 3D oriented L-alanine microcrystals. The chemical shift of the  $\text{COO}^-$  peak coincided with that of the SC rotation pattern at  $\theta = 90^\circ$  (see Fig. 4). Fig. 6 shows the change in the full width at half maximum (FWHM) of the  $\text{COO}^-$  peaks between 100 and 724 s. The solid line shows a fitting curve using an exponential function  $f(t) = C_0 + C \exp(-t/\tau)$ , where  $C_0 = 17.9$ ,  $C = 22.2$ , and  $\tau = 76.5$  s. The  $\tau$  value is related to the time required for orientation of the  $\chi_3$ -axes under the intermittent rotating magnetic field and is inversely proportional to  $K_1(\chi_2 - \chi_3)$  and  $K_2(\chi_1 - \chi_3)$  in Eq. (1). The constants  $K_1$  and  $K_2$  for the case of the intermittent mode used in the present study are determined as  $K_1 = 1/3$  and  $K_2 = 2/3$  [14]. Using the values of  $\chi_2 - \chi_3 = 3.0 \times 10^{-7}$  and  $\chi_1 - \chi_3 = 6.0 \times 10^{-7}$ , we find that  $\tau$  values are 18.2 and 4.6 s, which are smaller than the experimental value of 76.5 s. The reason for this discrepancy is not clear at present. We found that intermittent rotation for several minutes is required for the present L-alanine microcrystal suspension. Considering that it should take several times  $\tau$  before the steady state is established, full alignment attained by intermittent rotation for several minutes is reasonable.

It should also be noted that the microcrystals aligned magnetically have orientation fluctuation even after exposed to the magnetic field for a longer time under RRR condition. Under the intermittent rotation with RRR condition, the FWHM values decreased with the exposure time and finally reached to ca. 18 ppm. This value is larger than the linewidth (estimated as ca. 5 ppm) of L-alanine SC [24]. This is mainly ascribed to the orientation fluctuation due to the thermal fluctuation. The in situ measurements of 3D-MOMS at lower temperature may reduce the

thermal fluctuation, resulting in smaller linewidths of the resonance peaks. The combination of MOMS probe with a variable temperature unit may be a powerful tool to obtain sharp resonance peaks of 3D-MOMS.

## 5. Conclusions

A probe to measure solid-state NMR spectra of a MOMS was developed to realize the in situ measurements of aligned microcrystals dispersed in a liquid. The SC rotation patterns were successfully obtained from the microcrystals aligned three-dimensionally under an intermittently rotating magnetic field. The spectral changes during the 3D magnetic alignment of the  $^{13}\text{C}$ -labelled microcrystals were also observed. Our results demonstrated that the SC rotation pattern of microcrystals in a liquid medium can be directly obtained without solidification of the medium. The developed probe enables the experimental evaluation of the anisotropic interaction tensors of rare and/or minute crystalline samples originating from various fields such as organic/inorganic chemistry, structural biology, and pharmacy, provided that the sample is a biaxial crystal with micrometer size. This probe also facilitates the application of the traditional, most accurate SC method because the probe does not require the adjustment of the direction of the reference frame, which is time-consuming and often impossible for micrometer-scale crystals. A probe that enables the direction of the modulated-rotation axis to be changed rapidly is being developed to achieve the complete determination of anisotropic interaction tensors from 3D-MOMSs.

## Acknowledgments

This work was partially supported by a Grant-in-Aid for Scientific Research C (No. 17K05882) from the Japan Society for the Promotion of Science (JSPS) and the Advanced Low Carbon Technology Research and Development Program (ALCA; JPMJAL1502) of the Japan Science and Technology Agency (JST).

## Appendix A. Supplementary material

Supplementary data to this article can be found online at <https://doi.org/10.1016/j.jmr.2019.106618>.

## References

- [1] C.A. Fyfe, *Solid State NMR for Chemists*, C.F.C. Press, Guelph, 1983.
- [2] M.H. Sherwood, Chemical shift tensors in single crystals, in: D.M. Grant, R.K. Harris (Eds.), *Encyclopedia of Nuclear Magnetic Resonance*, John Wiley & Sons, Chichester, 1996, pp. 1322–1330.
- [3] R. Blinc, J. Petkovšek, I. Zupančič,  $\text{Na}^{23}$  magnetic-resonance study of the ferroelectric transition in rochelle salt, *Phys. Rev.* 136 (1964) A1684–A1692.
- [4] C.M. Carter, D.W. Alderman, D.M. Grant, Two-dimensional chemical-shift anisotropy correlation spectroscopy. Measurements in complex single crystals, *J. Magn. Reson.* 73 (1987) 114–122.
- [5] M.H. Sherwood, D.W. Alderman, D.M. Grant, Two-dimensional chemical-shift tensor correlation spectroscopy. Multiple-axis sample-reorientation mechanism, *J. Magn. Reson.* 84 (1989) 466–489.
- [6] A.P.M. Kentgens, J. Bart, P.J.M. van Bentum, A. Brinkmann, E.R.H. van Eck, J.G.E. Gardeniers, J.W.G. Janssen, P. Knijn, S. Vasa, M.H.W. Verkuijlen, High-resolution liquid- and solid-state nuclear magnetic resonance of nanoliter sample volumes using microcoil detectors, *J. Chem. Phys.* 128 (2008) 052202.
- [7] G.H. Kunath-Fandrei, L. Kelbauskas, D. Döring, H. Rager, C. Jäger, Determination of the orientation of  $^{29}\text{Si}$  chemical shift tensors using rotorsynchronized MAS NMR of single crystals: forsterite ( $\text{Mg}_2\text{SiO}_4$ ), *Phys. Chem. Minerals* 26 (1998) 55–62.
- [8] S.K. Vasa, E.R.H. van Eck, J.W.G. Janssen, A.P.M. Kentgens, Full quadrupolar tensor determination by NMR using a micro-crystal spinning at the magic angle, *Phys. Chem. Chem. Phys.* 12 (2010) 4813–4820.
- [9] R. Kusumi, F. Kimura, G. Song, T. Kimura, Chemical shift tensor determination using magnetically oriented microcrystal array (MOMA):  $^{13}\text{C}$  solid-state CP NMR without MAS, *J. Magn. Reson.* 223 (2012) 68–72.

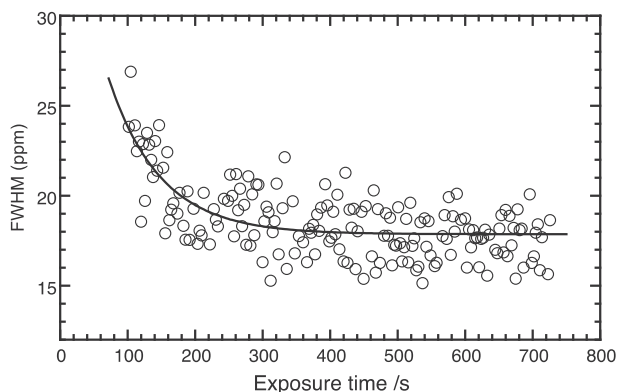


**Fig. 6.** Plots of the full width at half maximum (FWHM) values of the  $^{13}\text{C}$  resonance peaks in Fig. 5 as a function of the time exposed to the intermittent rotating magnetic field between 100 and 724 s. The FWHM values were obtained from fitting with a Gaussian function.

- [10] R. Kusumi, F. Kimura, T. Kimura, Determination of  $^{31}\text{P}$  chemical shift tensor from microcrystalline powder by using a magnetically oriented microcrystal array, *Cryst. Growth Des.* 15 (2015) 718–722.
- [11] G. Song, R. Kusumi, F. Kimura, T. Kimura, K. Deguchi, S. Ohki, T. Fujito, T. Simizu, Single-crystal NMR approach for determining chemical shift tensors from powder samples via magnetically oriented microcrystal arrays, *J. Magn. Reson.* 255 (2015) 28–33.
- [12] T. Kimura, F. Kimura, M. Yoshino, Magnetic alteration of crystallite alignment converting powder to a pseudo single crystal, *Langmuir* 22 (2006) 3464–3466.
- [13] T. Kimura, M. Yoshino, Three-dimensional crystal alignment using a time-dependent elliptic magnetic field, *Langmuir* 21 (2005) 4805–4808.
- [14] F. Kimura, T. Kimura, Magnetically textured powders—an alternative to single-crystal and powder X-ray diffraction methods, *CrystEngComm* 20 (2018) 861–872.
- [15] M. Yamaguchi, S. Ozawa, I. Yamamoto, T. Kimura, Characterization of three-dimensional magnetic alignment for magnetically biaxial particles, *Jpn. J. Appl. Phys.* 52 (2013) 013003.
- [16] M. Staines, New Zealand Pat. (1995) 28163.
- [17] J.-Y. Genoud, M. Staines, A. Mawdsley, V. Manojlovic, W. Quinton, Biaxially textured YBCO coated tape prepared using dynamic magnetic grain alignment, *Supercond. Sci. Technol.* 12 (1999) 663–671.
- [18] M. Yamaki, S. Horii, M. Haruta, J. Shimoyama, Rare-earth-dependent tri-axial magnetic anisotropies and growth conditions in  $\text{REBa}_2\text{Cu}_4\text{O}_8$ , *Jpn. J. Appl. Phys.* 51 (2011) 010107.
- [19] N. Nakatsuka, H. Yasuda, T. Nagira, M. Yoshiya, Three-dimensional alignment of  $\text{FeSi}_2$  with orthorhombic symmetry by an anisotropic magnetic field, *J. Phys.: Conf. Ser.* 165 (2009) 012021.
- [20] T. Kimura, Orientation of feeble magnetic particles in dynamic magnetic fields, *Jpn. J. Appl. Phys.* 48 (2009) 020217.
- [21] T. Kimura, M. Yamato, W. Koshimizu, M. Koike, T. Kawai, Magnetic orientation of polymer fibers in suspension, *Langmuir* 16 (2000) 858–861.
- [22] C. Tsuboi, S. Tsukui, F. Kimura, T. Kimura, K. Hasegawa, S. Baba, N. Mizuno, X-ray diffraction from magnetically oriented microcrystal suspensions detected by a shutterless continuous rotation method, *J. Appl. Cryst.* 49 (2016) 2100–2105.
- [23] K. Takeda, OPENCORE NMR: Open-source core modules for implementing an integrated FPGA-based NMR spectrometer, *J. Magn. Reson.* 192 (2008) 218–229.
- [24] A. Naito, S. Ganapathy, K. Akasaka, C.A. McDowell, Chemical shielding tensor and  $^{13}\text{C}$ – $^{14}\text{N}$  dipolar splitting in single crystals of L-alanine, *J. Chem. Phys.* 74 (1981) 3190–3197.
- [25] H.J. Simpson, R.E. Marsh, The crystal structure of L-alanine, *Acta Cryst.* 20 (1966) 550–555.
- [26] K. Matsumoto, F. Kimura, S. Tsukui, T. Kimura, X-ray diffraction of a magnetically oriented microcrystal suspension of L-alanine, *Cryst. Growth Des.* 11 (2011) 945–948.